Clinical Cancer Research

Long Noncoding RNA *NEAT1*, Regulated by the EGFR Pathway, Contributes to Glioblastoma Progression Through the WNT/β-Catenin Pathway by Scaffolding EZH2

Qun Chen[1,2,3], Jinquan Cai[1,2,3], Qixue Wang[3,4], Yunfei Wang[3,4], Mingyang Liu[5], Jingxuan Yang[5], Junhu Zhou[3,4], Chunsheng Kang[3,4], Min Li[5], and Chuanlu Jiang[1,2,3]

Abstract

Purpose: Long noncoding RNAs have been implicated in gliomagenesis, but their mechanisms of action are mainly undocumented. Through public glioma mRNA expression data sets, we found that *NEAT1* was a potential oncogene. We systematically analyzed the clinical significance and mechanism of *NEAT1* in glioblastoma.

Experimental Design: Initially, we evaluated whether *NEAT1* expression levels could be regulated by EGFR pathway activity. We subsequently evaluated the effect of *NEAT1* on the WNT/β-catenin pathway and its target binding gene. The animal model supported the experimental findings.

Results: We found that *NEAT1* levels were regulated by EGFR pathway activity, which was mediated by STAT3 and NFκB (p65) downstream of the EGFR pathway. Moreover, we found that *NEAT1* was critical for glioma cell growth and invasion by increasing β-catenin nuclear transport and downregulating ICAT, GSK3B, and Axin2. Taken together, we found that *NEAT1* could bind to EZH2 and mediate the trimethylation of H3K27 in their promoters. *NEAT1* depletion also inhibited GBM cell growth and invasion in the intracranial animal model.

Conclusions: The EGFR/*NEAT1*/EZH2/β-catenin axis serves as a critical effector of tumorigenesis and progression, suggesting new therapeutic directions in glioblastoma. *Clin Cancer Res; 24(3); 684–95.* *©2017 AACR.*

Introduction

Glioma is the most common and malignant tumor in the central nervous system. Maximal safe resection following radiotherapy and chemotherapy is the most popular therapeutic regimen for patients who have a malignant brain tumor. However, the overall survival of glioblastoma (GBM) patients is approximately 15 months from the time of diagnosis (1). EGFR alteration is an important marker in glioblastoma. EGFRvIII, the most common EGFR mutant, is found in 50%–60% cases, strongly indicating a poor survival prognosis (2–4). In 2014, EGFR module (EM)/PDGFRA (platelet-derived growth factor receptor A) (PM)-based molecular classification was performed and provided a molecular diagnostic framework to expedite the search for new glioma therapeutic targets (5). Furthermore, the molecular mechanism underlying glioma progression remains poorly understood. Therefore, a better understanding of gliomagenesis and progression are essential for the development of diagnostic markers and novel effective therapies for glioma patients. Long noncoding RNAs, nonprotein coding transcripts longer than 200 nucleotides, have recently emerged as critical regulators of gene expression. Bromodomain protein BRD4 promotes the expression of *HOTAIR* to regulate the cell cycle of glioma cells (6). In a hypoxic microenvironment, *HIF1A-AS2* facilitates the maintenance of mesenchymal glioblastoma stem-like cells (7). A lncRNA transcribed from the 5-prime end of the HOXA transcript *HOXA11-AS* contributes to the malignant progression of glioblastoma (8). In this study, we compared the lncRNA profiles of glioma tissues from different grades using RNA microarrays from the CGGA, Rembrandt, TCGA, and GSE16011 projects. We discovered that nuclear enriched abundant transcript 1 (*NEAT1*) displayed specific overexpression in the EGFR module, but not in the PDGFR module. *NEAT1* is an abundant intranuclear lncRNA containing two transcripts, *NEAT1_1* (3.7 kb) and *NEAT1_2* (23 kb), and the latter is a core component of paraspeckles, which is a major

[1]Department of Neurosurgery, the Second Affiliated Hospital of Harbin Medical University, Harbin, China. [2]Neuroscience Institute, Heilongjiang Academy of Medical Sciences, Harbin, China. [3]Glioma Cooperative Group (CGCG), Beijing, China. [4]Department of Neurosurgery, Laboratory of Neuro-oncology, Tianjin Neurological Institute, Key Laboratory of Post-Neuro Injury Neuro-repair and Regeneration in Central Nervous System, Ministry of Education, Tianjin Medical University General Hospital, Tianjin, China. [5]Department of Medicine, Department of Surgery, University of Oklahoma Health Sciences Center, Oklahoma City, Oklahoma.

Note: Supplementary data for this article are available at Clinical Cancer Research Online (http://clincancerres.aacrjournals.org/).

Q. Chen and J. Cai contributed equally to this article.

Corresponding Authors: Chuanlu Jiang, The Second Affiliated Hospital of Harbin Medical University, No. 246, Xuefu Road, Nangang District, 150086, Harbin, China. Phone: 8645-1866-05088; Fax: 8645-1866-05461; E-mail: jcl6688@163.com; Min Li, University of Oklahoma Health Sciences Center, 975 Northeast 10th Street, BRC 1262A, Oklahoma City, OK 73104. Phone: 405-271-1796; Fax: 405-271-1476; E-mail: Min-Li@ouhsc.edu; and Chunsheng Kang, Laboratory of Neuro-oncology, Tianjin Neurological Institute, Tianjin Medical University General Hospital, Tianjin 300052, China. Phone: 8622-6081-7499; Fax: 8622-2781-3550; E-mail: kang97061@tmu.edu.cn

doi: 10.1158/1078-0432.CCR-17-0605

Translational Relevance

The highly proliferative and invasive hallmarks of glioblastoma account for its dismal prognosis. Despite thousands of studies into overcoming the proliferation and invasion of glioblastoma, little progress has been made, and the underlying mechanisms of glioblastoma tumorigenesis remain poorly understood. This is the first report of the EGFR/*NEAT1*/EZH2/β-catenin axis in glioblastoma, in which *NEAT1* levels are regulated by EGFR pathway activity and are critical for glioma cell growth and invasion through the WNT/β-catenin pathway by scaffolding EZH2 and mediating the H3K27 trimethylation of three WNT/β-catenin pathway negatively regulated factor (Axin2, ICAT, and GSK3B) promoter regions. This finding unmasks the oncogenic function that *NEAT1* driven by EGFR activity recapitulates the early embryonic developmental signaling pathway (WNT/β-catenin pathway) and offers *NEAT1*-based therapeutic targets in glioblastoma.

complex in RNA nuclear retention that participates in precursor RNA splicing (9). Both *NEAT1_1* and *NEAT1_2* are induced in an anoxic environment (10). A recent study reports that p53 induces the formation of *NEAT1* lncRNA-containing paraspeckles that modulate the replication stress response and chemosensitivity (11). *NEAT1* is also a p53-dependent lncRNA in chronic lymphocytic leukemia (12). *NEAT1* can also be induced by poly I:C triggered by the toll-like receptor3-p38 pathway after infection with virus (13). Previous studies have shown that *NEAT1* is an oncogene in various cancers, such as urinary bladder cancer, colorectal cancer, and nasopharyngeal carcinoma (14–17). In addition to lncRNA, many tumor pathways have been shown to play an important role in glioma progression and invasion. Abnormal activation of the canonical WNT/β-catenin pathway has been reported to participate in malignant progression and has been implicated in the poor prognosis of malignant tumors (18) by regulating multiple aspects of cancer formation and growth. Axin2, GSK3B, and ICAT (CTNNBIP1), as WNT/β-catenin negatively regulated factors, play an important part in the canonical WNT/β-catenin pathway by promoting the degradation of β-catenin and repressing T-cell factor/lymphoid enhancer factor (TCF/LEF)–β-catenin transcriptional activity *in vitro* (19–21). However, the relationship between *NEAT1* and the WNT/β-catenin pathway is rarely reported. In this study, we found that the EGFR/*NEAT1*/EZH2/β-catenin axis, conferring an oncogenic function in glioblastoma, might be a novel therapeutic target in glioblastoma.

Materials and Methods

Atlases of glioma samples

MRNA expression data sets and the associated clinical information were downloaded from the following websites: CGGA (http://www.cgga.org.cn), Rembrandt (http://caintegrator.nci.nih.gov/rembrandt/), GSE16011 (http://www.ncbi.nlm.nih.gov/geo/query/acc.cgi?acc=GSE16011), and TCGA (http://cancergenome.nih.gov/). DNA methylation and copy number data of GBM were downloaded from TCGA website (http://xena.ucsc.edu/getting-started/). The population characteristics of the 4 data sets are in Supplementary Tables S1 to S4.

Cell culture and treatments

N5, N9, and N33 patient-derived cells were obtained from Professor Fan from BNU Beijing Normal University. N5, N9, and N33 cells were grown in DMEM/F12 (1:1; Gibco) and supplemented with 10% FBS and 1% penicillin–streptomycin. Cells were grown at 37°C in 5% CO_2. For cell treatments in several experiments, 15 ng/mL EGF was mixed with DMEM/F12 (1:1) without 10% FBS for 24 hours. All glioblastoma cells except *in vivo* cultures were maintained for less than eight passages. Sequencing and clinical data are listed in Supplementary Tables S5 and S6.

Lentivirus, siRNA, sgRNAs, and transfection

Lentiviruses, such as Cas9, GFP vector, RFP vector, and luciferase lentivirus, which were for *in vivo* experiments, were obtained from Genechem. Lentivirus such as EGFRvIII, *HOTAIR*, *HOTAIR* 5′ domain, and the *HOTAIR* 5′ domain mutant were purchased from Shanghai Genepharma. siRNAs for EZH2 were purchased from Shanghai Genepharma. sgRNAs for *NEAT1* were purchased from Shanghai Genepharma. All sequences are provided in Supplementary Tables S7 and S8.

Cell proliferation assay, colony formation assay, cell invasion assay, and cell apoptosis assay

The CCK8 (Cell Counting Kit-8) assay was used to evaluate cell proliferation. Cells were seeded at 2×10^2 cells per well in 96-well plates. CCK8 was added at 0-, 24-, 48-, 72-, and 96-hour time-points. For colony formation assays, 250 cells were seeded in each well of six-well plates and were incubated for 14 days. The colonies were fixed with 4% paraformaldehyde, stained with crystal violet and counted. Invasion assays were performed using Boyden chambers (Corning) and 8-μm-sized pore membranes coated with Matrigel. Glioblastoma cells transfected with sgRNA or scramble were harvested 48 hours after transfection by 0.25% trypsinization. After the double staining with FITC-Annexin V and propidium iodide (PI), the cells were analyzed with flow cytometry (FACScan; BD Biosciences) equipped with CellQuest software (BD Biosciences).

RNA extraction and quantitative real-time PCR assays

Total RNA was extracted using TRIzol reagent (Sigma). The nuclear and cytoplasmic components were separated using 0.5% NP-40 (Solarbio) with an RNAase inhibitor (Promega), followed by extraction using TRIzol reagent (Sigma). Thereafter, cDNAs were synthesized using the PrimeScript RT Reagent Kit (Promega) according to the manufacturer's instructions. qRT-PCR was conducted in triplicate with LightCycler2.0 (Bio-Rad), and the expression was normalized to *GAPDH* as the total RNA and cytoplasmic RNA endogenous control. *U6* was used as the nuclear RNA endogenous control. PCR primers were designed and synthesized using a primer designing tool (http://www.ncbi.nlm.nih.gov/tools/primer-blast/), and the primer sequences are listed in Supplementary Table S9. The relative quantification value for each target gene was expressed as $2-\Delta\Delta C_t$.

Luciferase reporter assay

The pGL4.49[luc2P/TCF-LEF RE/Hygro] vector was purchased from Promega. The vectors were transfected into N5, N9, and N33 cells, and vector *Renilla* luciferase (Promega) served as an internal control. After 48 hours, cells were lysed and luciferase activities were measured using the Dual Luciferase Assay Kit (Promega) following the manufacturer's instructions.

GPCR (genome PCR) assay

Total genomic DNA was extracted using the TIAN amp Genomic DNA Kit (Tiangen). Conventional PCR and gPCR were performed using the Bio-Rad system, and 1% agarose gel electrophoresis (AGE) was used to detect the PCR products.

Western blot assay

Western blot analysis was performed according to the manufacturer's instructions as previously described (22). Primary antibodies rabbit anti-p53, anti-PDGFR, anti-EGFR, rabbit anti-EGFRvIII, rabbit anti-β-catenin, rabbit anti-phospho-β-catenin (Ser675), mouse anti-H3, rabbit anti-Axin2, rabbit anti-EZH2, rabbit anti-STAT3, rabbit anti-Phospho-STAT3 (Ser705), rabbit anti-NF-κB (p65), and rabbit anti-phospho-NF-κB (p65) (Ser536) were purchased from Cell Signaling Technology. Primary antibodies rabbit anti-ICAT and mouse anti-GSK3B were purchased from Abcam. Primary antibody rabbit anti-TCF-4 was purchased from Santa Cruz Biotechnology. Mouse anti-GAPDH antibody was purchased from ProteinTech.

Coimmunoprecipitation assay

The cells were lysed using Western and IP lysis buffer (Beyotime Biotechnology) and incubated with 40 μL of protein-A/G PLUS-Agarose beads (Millipore), 1 μg of rabbit anti-β-catenin (Cell Signaling Technology), and anti-TCF-4 (Santa Cruz Biotechnology) at 4°C overnight. After washing three times with RIPA buffer, the samples were analyzed by Western blot analysis.

Immunofluoresence assay

Antibodies against phospho-β-catenin (Ser675), β-catenin, and ICAT (1:300 dilution) and the secondary antibodies Alexa Fluor 488 and 594 (Life Technologies Corp.) were employed in immunofluoresence staining. Microscopy analysis was performed using an FV-1200 laser scanning confocal microscope.

Chromatin immunoprecipitation assay

All chromatin immunoprecipitation (ChIP) experiments were executed using the Millipore EZ-Magna ChIP Kit (catalog no. 17-371). Briefly, 2–3 $\times$ 10^5 cells were cross-linked with 1% formaldehyde for 10 minutes at room temperature. The cross-linking was then quenched with 10 $\times$ glycine. Chromatin was sonicated in lysis buffer to 200–1,000 bp, and the extraction of ChIP DNA was performed as per the kit's protocol. The antibodies utilized included H3K27Me3, STAT3, and NFκB (p65) (Cell Signaling Technology, 1:50 dilution). The primer sequences are given in Supplementary Table S9.

RNA binding protein immunoprecipitation and RIP-qPCR assays

RNA binding protein (RBP) immunoprecipitation (RIP) experiments were performed using the RNA Immunoprecipitation Kit (BersinBi) according to the manufacturer's instructions. Rabbit anti-EZH2 and anti-DNMT1 antibodies (1:50; Cell Signaling Technology) were used for experiments. Lysates were incubated with the antibody for 4 hours in 4°C. The coprecipitated RNAs were detected by real-time PCR.

Chromatin isolation using the RNA purification assay

Chromatin isolation using the RNA purification (ChIRP) experiments were performed using the ChIRP Kit (BersinBi). Complementary DNA oligonucleotides against *NEAT1* were constructed using BLAST and 3′-end biotinylated to capture DNA–RNA hybrids on streptavidin-coated magnetic beads. Cells were incubated in 1% glutaraldehyde and were then rinsed with phosphate-buffered saline. Probes (100 pmol) were added to 1 mg of precleared chromatin and were mixed by end-to-end rotation at 65°C for 10 minutes, 25°C for 30 minutes, 50°C for 5 minutes, and 25°C for 90 minutes. The beads were resuspended in 95 μL of RNA PK buffer at pH 7.0. Next, 5 μL of proteinase K was added and incubated at 50°C for 45 minutes with end-to-end shaking, and Trizol reagent was used to collect RNA. For protein, 100 μL of washed/blocked streptavidin magnetic beads were added to the samples (30 minutes). The beads were treated with Urea CHAPS buffer for 1 hour at room temperature, and proteins were analyzed by Western blot analysis. Sequences of biotin probes were listed in Supplementary Table S10.

In situ* hybridization histochemistry for *NEAT1

In situ hybridization histochemistry (RNA ISH) experiments were performed using the RNA *In Situ* Hybridization Kit (BersinBi) according to the manufacturer's instructions. Briefly, glioblastoma cells were fixed in 4% paraformaldehyde for 20 minutes and washed with distilled water. Fixed cells were treated with pepsin (1% in 10 mmol/L HCl), and the cells were further incubated with 20 nmol/L ISH probe in hybridization buffer (100 mg/mL dextran sulfate, 10% formamide in 2 $\times$ SSC) at 90°C for 3 min. Hybridization was performed at 37°C for 18 hours, and the slide was washed and incubated with digoxin antibodies for 1 hour. Finally, the slide was mounted with diaminobenzidine (DAB) for detection. RNA ISH probes were designed and synthesized by BersinBi, and the probe sequence is listed in Supplementary Table S8.

Nude mouse intracranial model, H&E staining, and immunohistochemistry assays

BALB/c-A nude mice at 3 to 4 weeks of age were purchased. To establish the intracranial tumor model, 3 $\times$ 10^5 N33 cells were separately implanted stereotactically using cranial guide screws. Bioluminescence imaging was used to detect intracranial tumor growth mice on days 7, 14, and 21. In the meantime, overall mouse survival time was monitored. Twenty-five days after implantation, mice were randomly sacrificed in each group. The brains of the mice were carefully extracted and fixed in 10% formalin. Next, they were embedded in paraffin for hematoxylin and eosin (H&E) and IHC. At the end of the experiment, all the mice were dead, and the mouse overall survival curves were recorded according to the Kaplan–Meier method. In addition, 3 $\times$ 10^5 mixed cells labeled with GFP and RFP were implanted stereotactically. After 21 days, brains of the mice were carefully extracted, fixed in 10% formalin and dehydrated in 30% sucrose. Next, they were embedded in optimal cutting temperature (OCT compound) and sliced for microscope observation.

Statistical analysis

The chi-squared test was used to determine whether there was a significant difference between the two groups. Survival curves were drawn using Kaplan–Meier survival plots, and the log-rank test was used to test significance. The correlation in tissues was examined using two-sided Pearson correlation. Statistical significance was determined using Student *t* test or ANOVA for functional analysis. Pathway and GO analysis were performed using DAVID (http://david.abcc.ncifcrf.gov/). Heat maps were constructed using Gene Cluster 3.0 and Gene Tree View software. Gene Set Enrichment Analysis (GSEA) was used. All statistical analysis were performed using SPSS 22.0 software and GraphPad Prism 6. The error bars in the figures represented SD. A P value < 0.05 was regarded as statistically significant.

Results

NEAT1 can be induced by EGFR pathway activity

To identify the lncRNAs that were involved in gliomagenesis, we selected 202 lncRNAs, most of which were according to Chiara Pastori, Zhou Du, and Brian J. Reon (6, 23, 24) and overlapped with glioma genome atlas public databases, such as the CGGA, Rembrandt, TCGA, and GSE16011 data sets (Fig. 1A). We placed these overlapping lncRNAs into the CGGA ($n = 81$), Rembrandt ($n = 474$), TCGA ($n = 702$), and GSE16011 ($n = 246$) data sets and classified them based on EM/PM (5). Next, we found that the *NEAT1* lncRNA was highly expressed in the EM in the CGGA, Rembrandt, TCGA, and GSE16011 data sets (Fig. 1B). The ROCs of four data sets indicated that *NEAT1* belonged to the EGFR module (Supplementary Fig. S1A). Status of EGFR (or EGFRvIII), p53, and PDGFR were validated through Western blot analysis, as shown in Supplementary Fig. S1B. Thus, we hypothesized that *NEAT1* could be induced by EGFR activity. Sequencing data of patient-derived cells were displayed (Fig. 1C). In our study, the *NEAT1_1* and *NEAT1_2* expression levels were higher in lenti-EGFRvIII and the EGF (15 ng/mL) stimulation groups than in the control groups in N5 and N9 cells (Fig. 1D). Compared with the control groups, the EGFRvIII and EGF stimulation groups showed elevated levels of p-STAT3 (Tyr705) and p-NF-κB (Ser536) (Fig. 1E). The ChIP assay showed that STAT3 and NF-κB could bind to the *NEAT1* promoter region (Fig. 1F). ChIP-qPCR showed that STAT3 and NF-κB binding activity were much higher in the lenti-EGFRvIII and EGF-stimulation groups than in the control groups (Fig. 1G). These results indicated that *NEAT1* could be regulated by EGFR pathway activity.

NEAT1-negative–associated genes are mainly enriched in the WNT/β-catenin pathway

To investigate the potential mechanisms of *NEAT1* in glioblastoma cells, correlation analysis was performed in 109 and 172 samples with GBM mRNA databases from the CGGA and TCGA, and a cluster ($|r| > 0.4$, $P < 0.01$) of *NEAT1*-associated genes was obtained (Fig. 2A). Next, pathway and GO analysis were performed. Pathway and GO analysis using the *NEAT1* positive correlation genes were conducted. We found that *NEAT1* was associated with EGFR-driven tumor signaling (Supplementary Fig. S1C and S1D). In the meantime, we found that the negative-associated gene expression profiles were associated with the WNT/β-catenin pathway (Fig. 2B and C). GSEA analysis showed that *NEAT1* negative-associated genes were primarily involved in the WNT/β-catenin signaling pathway (Fig. 2D). Further, correlation analysis revealed that the WNT/β-catenin negative regulatory factors *Axin2*, *ICAT*, and *GSK3B* had a significant negative correlation with *NEAT1* in the CGGA data set (Fig. 2E).

Knockdown of *NEAT1* using the dual CRISPR/Cas9 system inhibits proliferation, clone formation, and invasion but induces cell apoptosis in glioblastoma cells

LncRNAs have widely varying subcellular distributions; some reside predominantly in the nucleus, cytoplasm, or in both compartments. The RNAi-based gene-knockdown method is not effective to knockdown nuclear lncRNA (25). In our experiment, we proved that *NEAT1* was a nuclear-enriched abundant lncRNA in N5, N9, and N33 cells (Supplementary Fig. S2A). The CRISPR/Cas9 system has been reported to successfully knockdown various lncRNAs (26–28). Therefore, we designed a strategy to knockdown *NEAT1* by dual sgRNAs (Supplementary Fig. S2B). After sgRNAs infection of N5, N9 and N33 cells, we first amplified the dual-gRNA-targeted region by genomic PCR using primers outside of two gRNAs to confirm the knockdown of *NEAT1*. We next detected the deletion band (Supplementary Fig. S2C). qRT-PCR was then performed to detect *NEAT1* expression. The results demonstrated a substantial reduction of *NEAT1_1* and *NEAT1_2* in N5, N9 and N33 cells (Supplementary Fig. S2D). We used qRT-PCR to detect the *NEAT1_1* and *NEAT1_2* levels in the nucleus and cytoplasm, respectively, and found that *NEAT1_1* and *NEAT1_2* dramatically decreased according to the dual-sgRNA-CRISPR/Cas9 system both in the nucleus and cytoplasm (Supplementary Fig. S2E). *NEAT1* staining was attenuated in the nuclei of dual-sgRNA transfected cells, which highlighted that *NEAT1* was a nuclear-enriched abundant lncRNA in glioblastoma and could be inhibited by the CRISPR-Cas9 system (Supplementary Fig. S2F). The malignant behaviors of glioblastoma, including proliferation and invasion, were inhibited after *NEAT1* was knocked down (Supplementary Fig. S3A–S3C). To mimic the complexity of this heterogeneous disease, we used co-culture of scramble (e.g., GFP) with sgRNA1+2 group cells (e.g., RFP; for all three cells: N5, N9, N33) in an *in vitro* invasion assay. The results showed that *NEAT1* KO cells are less invasive in vitro (Supplementary Fig. S3D). Knockdown of *NEAT1* also induced cell apoptosis (Supplementary Fig. S3E).

Knockdown of *NEAT1* expression affects the WNT/β-catenin pathway *in vitro*

The WNT/β-catenin signal is transduced through several cytoplasmic relay components to β-catenin, which enters the nucleus and forms a complex with T-cell factor/lymphoid enhancer factor (TCF/LEF) to activate the transcription of WNT target genes (29). Correlation analysis implied that the expression of *NEAT1* was associated with the WNT/β-catenin negative regulatory factors Axin2, ICAT, and GSK-3B (Fig. 3A). ICAT has been reported to inhibit glioblastoma cell proliferation by suppressing WNT/β-catenin activity, which is significantly downregulated in high-grade glioma patients compared with normal brain and low-grade glioma patients (19). Axin2 participates in a negative feedback loop that could serve to limit the duration of the WNT/β-Catenin signal. GSK-3B phosphorylates β-catenin, thereby flagging it for recognition and destruction by the ubiquitin/proteasome machinery (30). The *NEAT1* knockdown group showed that the mRNA levels of *Axin2*, *ICAT*, and *GSK3B* were increased in N3, N5, and N9 cells (Fig. 3B; Supplementary Fig. S4A). The protein levels of Axin2, ICAT, and GSK3B were also increased in the

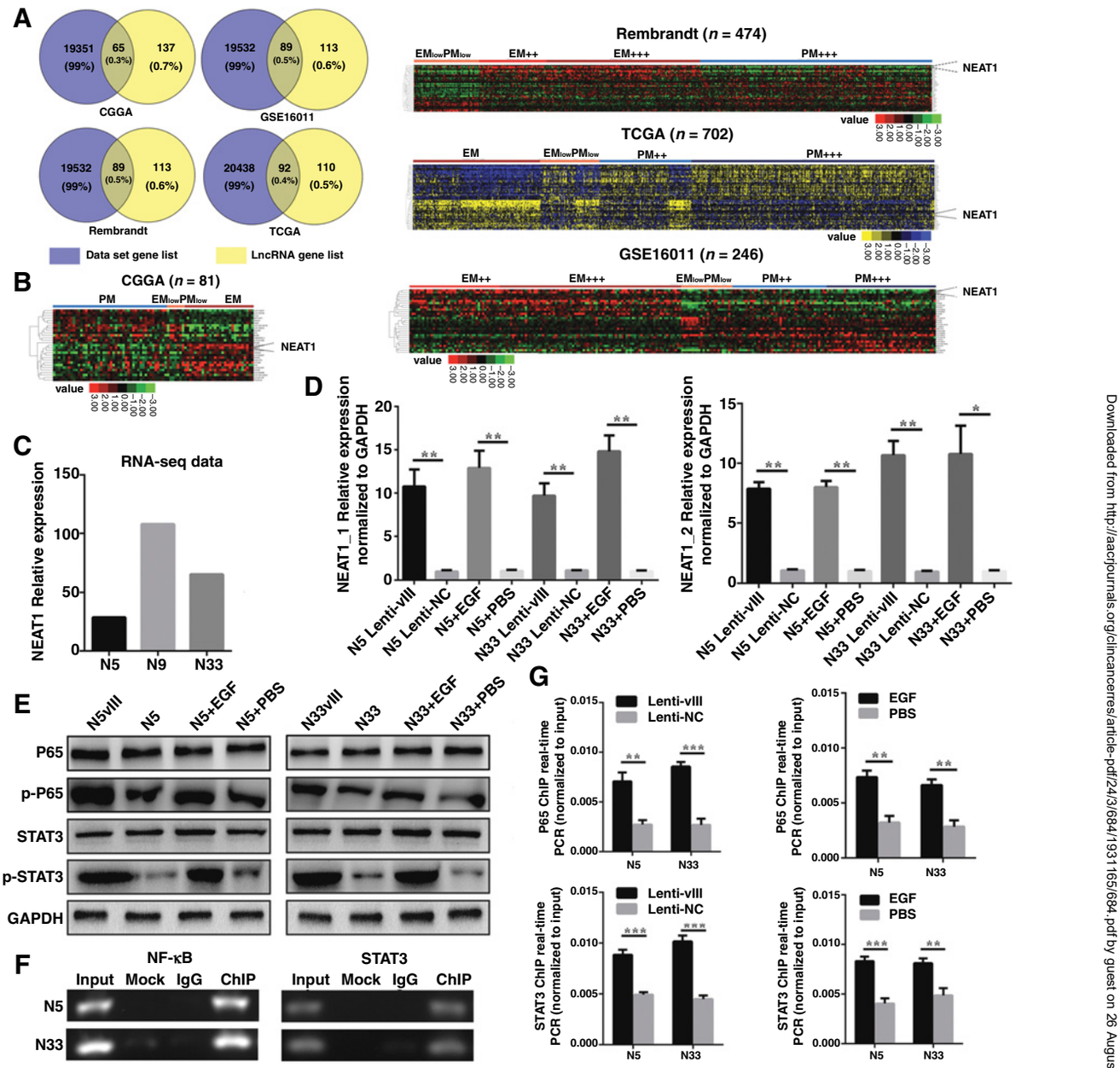

Figure 1.

NEAT1 could be driven by the activity of the EGFR pathway. **A,** Overlap of lncRNAs in the CGGA, Rembrandt, TCGA, and GSE16011 data sets. **B,** Hierarchical clustering analysis of lncRNAs that were differentially expressed in EM and PM glioma samples. **C,** *NEAT1* sequencing data of patient-derived cells. **D,** The *NEAT1_1* and *NEAT1_2* levels were detected in lenti-EGFRvIII, EGF stimulation, and control groups. **E,** The NF-κB, p-NF-κB (Ser536), STAT3, and p-STAT3 (Tyr705) protein levels of N9 and N33 were separately detected in the EGFRvIII, EGF stimulation, and control groups. **F,** ChIP-PCR showed that STAT3 and NF-κB occupied the *NEAT1* promoter region. **G,** ChIP-qPCR was used to detect the binding of STAT3 and NF-κB at the *NEAT1* promoter region in the EGFRvIII, EGF stimulation, and control groups. *, $P < 0.05$; **, $P < 0.01$; ***, $P < 0.001$.

downregulated *NEAT1* groups (Fig. 3C; Supplementary Fig. S4B). Confocal results showed that ICAT levels increased after knockdown of *NEAT1* (Fig. 3D; Supplementary Fig. S4C). Furthermore, the total protein levels of β-catenin and p-β-catenin (Ser675) were decreased in the *NEAT1* downregulated group (Fig. 3E; Supplementary Fig. S5A). The TCF-LEF reporter system was used to examine the activity of WNT signaling. Our results showed that downregulated *NEAT1* could attenuate WNT/β-catenin signaling activity (Fig. 3F; Supplementary Fig. S5B). In the meantime, we measured the cellular distribution of β-catenin and p-β-catenin (Ser675). Downregulated *NEAT1* triggered a reduction of nuclear β-catenin and p-β-catenin (Ser675; Fig. 3G; Supplementary

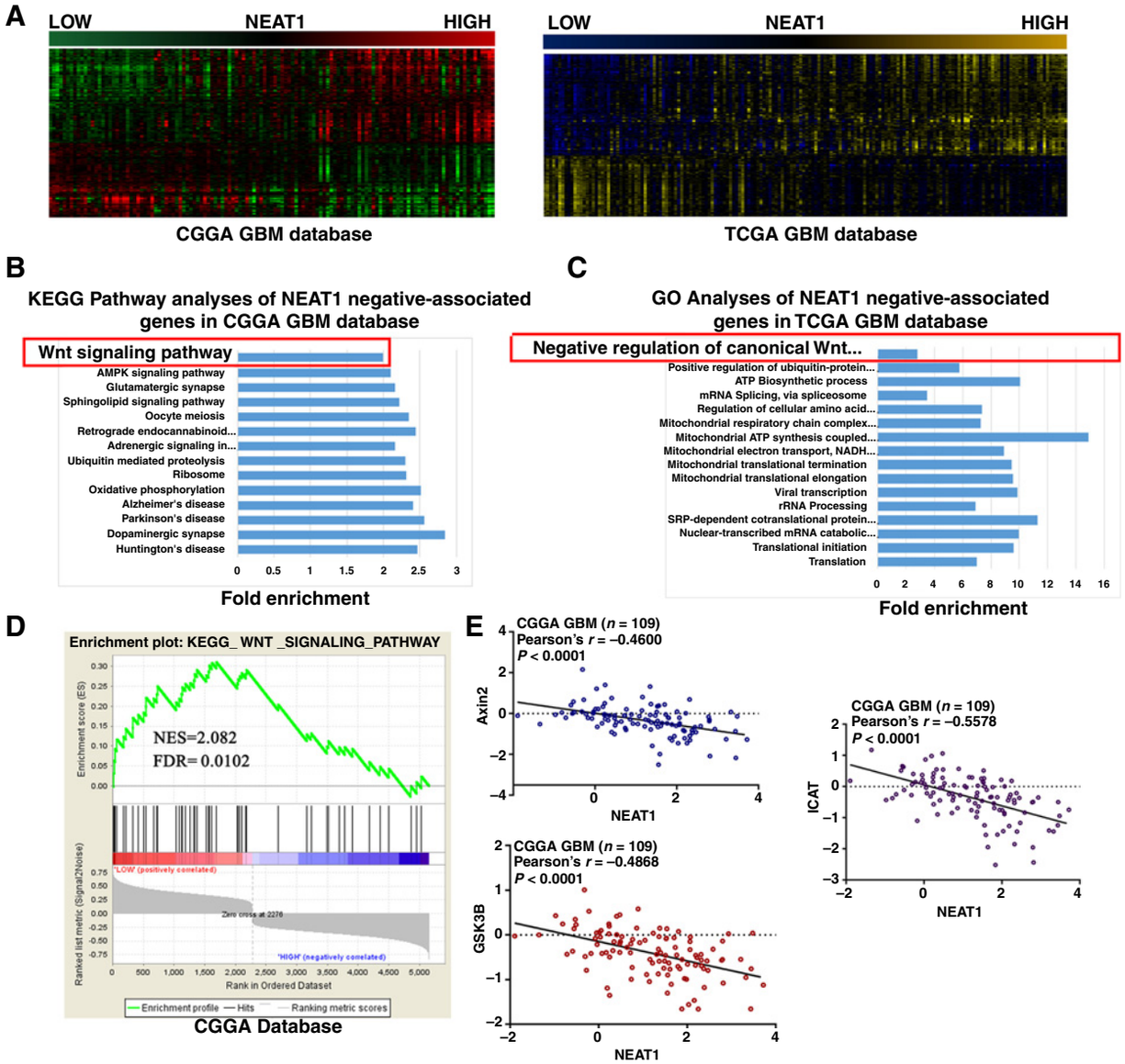

Figure 2.

NEAT1-associated genes are mainly enriched in the WNT/β-Catenin pathway. **A,** Heatmaps of *NEAT1*-associated genes in 109 and 172 glioblastoma tissues sorted by the level of *NEAT1* expression in CGGA and TCGA data sets. **B** and **C,** Pathway and GO analyses were performed using the NEAT1 negative-associated genes in CGGA and TCGA data sets. **D,** GSEA was performed in the CGGA data set. **E,** The correlation between *NEAT1* and *Axin2*, *ICAT*, and *GSK3B* expression was detected in the CGGA data set.

Fig. S5C). Moreover, the immunofluorescence results demonstrated that β-catenin and p-β-catenin (Ser675) expression in the nucleus and cytoplasm was markedly decreased after *NEAT1* was knocked down (Fig. 3H; Supplementary Fig. S5D). Coimmunoprecipitation assay verified that the *NEAT1* knockdown group was able to attenuate β-Catenin binding activity with TCF-4 (Fig. 3I; Supplementary Fig. S5E). The above results demonstrate that knockdown of *NEAT1* expression regulated WNT/β-catenin through repressing WNT/β-catenin pathway negative regulatory factors such as Axin2, ICAT, and GSK3B and helping β-catenin nuclear transport *in vitro*. Next, we performed Pearson correlation analysis for the association between *Axin2*, *ICAT*, and *GSK3B* methylation levels and *NEAT1* expression in glioblastoma. However, we did not find an obvious positive association between *NEAT1* and the methylation levels of the WNT/β-catenin–positive regulatory factors *Axin2*, *ICAT*, and *GSK3B* ($r < 0.2$, Supplementary Fig. S6A–S6C). Moreover, we observed that *NEAT1* expression did not have a negative correlation with gene copy numbers (Supplementary Fig. S6D–S6F). In this situation, we suspected that *NEAT1* may perform like a scaffold with histone-modifying enzymes to regulate Axin2, ICAT, and GSK3B expression.

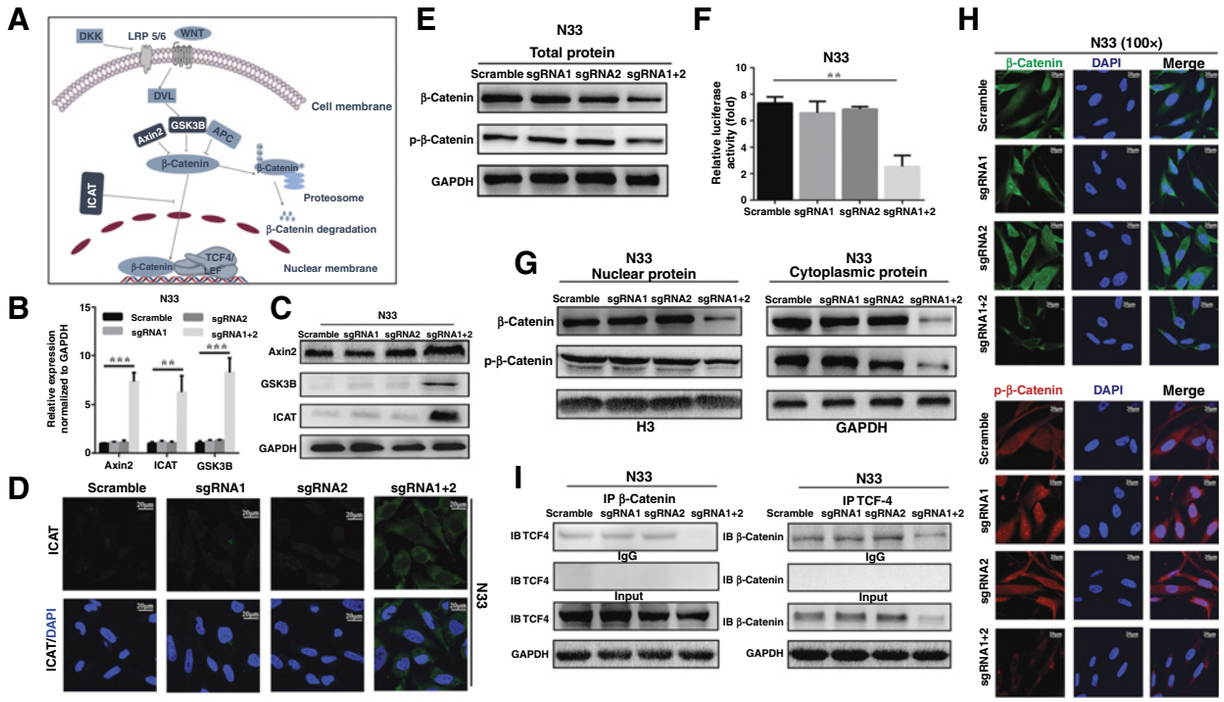

Figure 3.

Knockdown of *NEAT1* inhibits β-catenin by upregulating Axin2, ICAT, and GSK3B in N33 cells. **A,** In the bioinformatic analysis, *NEAT1*-associated downregulated genes were enriched in WNT/β-catenin pathway negative feedback factors. **B** and **C,** Axin2, ICAT, and GSK3B mRNA and protein levels were detected. **D,** ICAT level was detected through immunofluorescence assay. **E,** Total protein was used to detect the β-catenin and p-β-catenin level. GAPDH was used as a control in Western blot analysis. **F,** TCF luciferase reporter plasmid was used to test the activity of WNT/β-catenin pathway, and the expression was normalized to renilla activity. **G,** Cytoplasmic and nuclear proteins were extracted, and the β-catenin and p-β-catenin levels were detected. H3 was used as the nuclear control, and GAPDH was used as the cytoplasmic control. **H,** An immunofluorescence assay was used to detect the β-catenin and p-β-catenin levels and cellular distribution. **I,** A co-immunoprecipitation assay was used to detect binding activity between β-catenin and TCF-4. Scale bar, 20 μm. *, $P < 0.05$; **, $P < 0.01$; ***, $P < 0.001$.

NEAT1 interacts with EZH2

Evolutionary conservation is commonly used as an indicator of the functional significance of newly discovered genes. LncRNA conservation includes four dimensions: sequence, structure, function, and expression from syntenic loci (31). Through a sequence alignment analysis, we found that *NEAT1* was an evolutionarily conserved lncRNA (Supplementary Fig. S7A). Some lncRNAs affect the expression of protein-coding genes by interacting with the PRC2 subunit EZH2 (32–34). In starBase v2.0, we found that EZH2 in murine embryonic stem cells could bind to *Neat1* (http://starbase.sysu.edu.cn/; Supplementary Fig. S7B). In addition, we predicted the interaction probabilities of *NEAT1* and RBPs via RNA–protein interaction prediction (http://pridb.gdcb.iastate.edu/RPISeq/) and found that lncRNAs such as *HOTAIR* and *MALAT1* (metastasis associated with lung adenocarcinoma transcript 1), *NEAT1_1*, *NEAT1_2*, *Neat1_1*, and *Neat1_2* could potentially bind to EZH2 (Supplementary Fig. S7C). Thus, we hypothesized whether *NEAT1* could bind to EZH2 in glioblastoma cells. To investigate the potential interaction between lncRNA *NEAT1* and EZH2, RIP, and ChIRP (Fig. 4A), assays were carried out. We found that both *NEAT1_1* and *NEAT1_2* were significantly enriched with the EZH2 antibody compared with IgG (control antibody; Fig. 4B), but did not interact with DNMT1 (Supplementary Fig. S8A) in N9 and N33 cells; *HOTAIR* and *MALAT1* were used as positive controls. The downregulated *NEAT1* group attenuated *NEAT1*-binding activity (Fig. 4C). Moreover, the ChIRP results showed that *NEAT1* could be pulled out with biotinylated probes and was markedly enriched with EZH2 compared with the negative control (Fig. 4D and E). Next, we amplified *HOTAIR*, *HOTAIR* 5′ domain (35, 36), and *HOTAIR 5′* domain mutants (Supplementary Fig. S8B). We found no observable fold change in the expression of *MALAT1*, *NEAT1_1*, and *NEAT1_2* (Supplementary Fig. S8C). However, RIP experiments showed that the *HOTAIR* and *HOTAIR* 5′ domain overexpression groups impaired the binding activity of *NEAT1_1*, *NEAT1_2*, and *MALAT1* (Fig. 4F). These results further indicated that *NEAT1* was an EZH2-binding lncRNA.

NEAT1 leads to trimethylation of H3K27 in the promoter region of Axin2, ICAT, and GSK3B in glioblastoma

To reveal how *NEAT1* regulated WNT/β-catenin through EZH2, we separately designed three paired primers across the promoter region (2000 bp) of *Axin2*, *ICAT*, and *GSK3B* and then performed the ChIP-qPCR assay to examine the regulatory mechanisms. The results showed that knockdown of *NEAT1* group decreased the H3K27Me3 binding ability in N33 cells (Fig. 5A). Then, we knocked down EZH2 through siRNA and found that the β-catenin level decreased (Fig. 5B). RIP and ChIRP assays showed that the interactivity between *NEAT1* and EZH2 decreased in siEZH2 group (Fig. 5C and D). The mRNA and protein levels of Axin2,

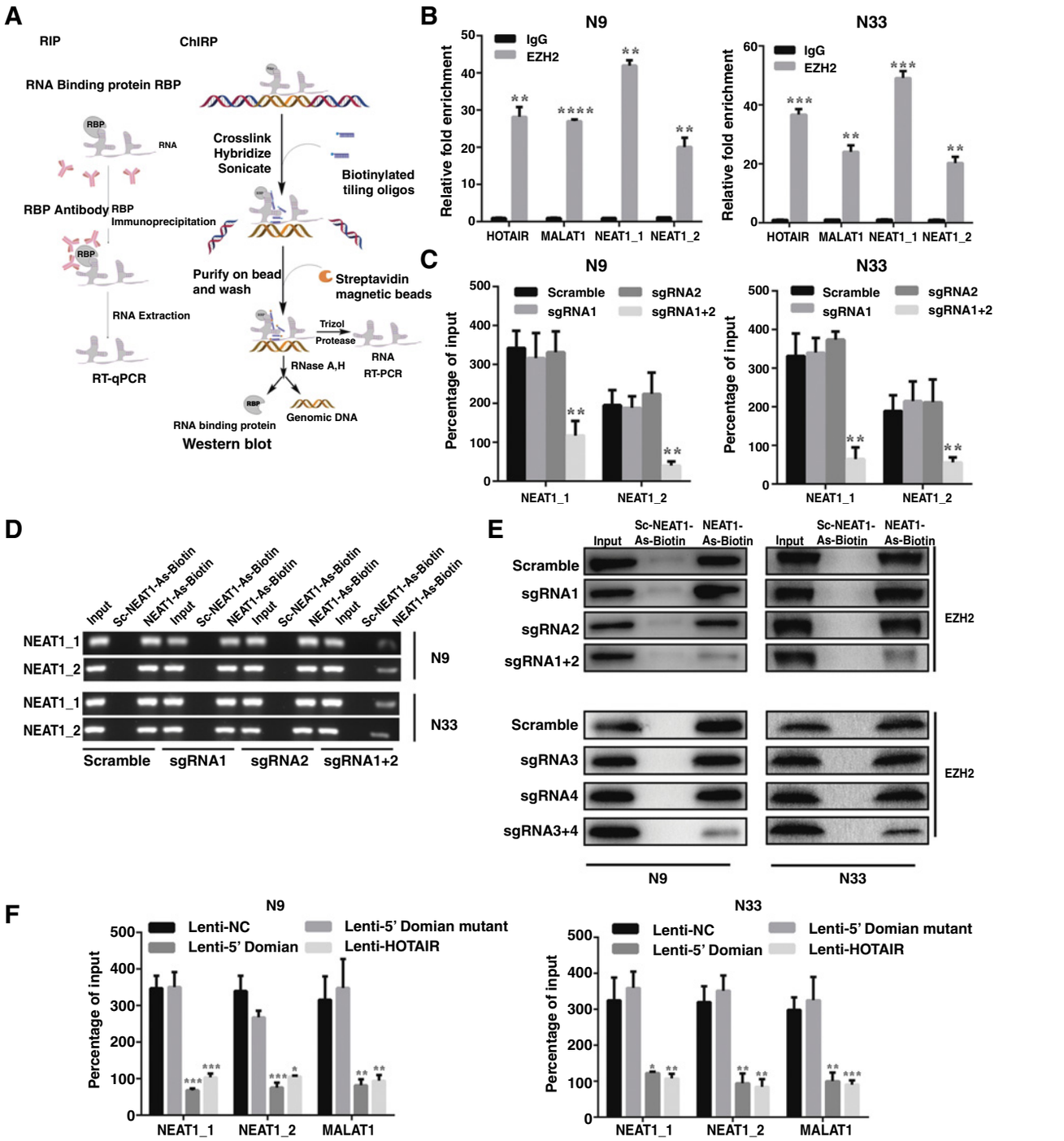

Figure 4.

NEAT1 interacts with EZH2 in glioblastoma cells. **A,** Technical route of RIP and ChIRP. **B,** *NEAT1* bound to EZH2 in N9 and N33 cell extracts; *HOTAIR* and *MALAT1* were used as the positive control. **C,** RIP assay was performed in different *NEAT1* treatment groups. **D,** ChIRP was used to examine the association of *NEAT1* in different *NEAT1* treatment groups. **E,** ChIRP was used to examine the association of EZH2 in different *NEAT1* treatment groups. **F,** The binding ability between *NEAT1_1*, *NEAT1_2*, *MALAT1*, and EZH2 was detected in the overexpression of *HOTAIR*, *HOTAIR* 5′ domain, and *HOTAIR* 5′ domain mutant groups. *, $P < 0.05$; **, $P < 0.01$; ***, $P < 0.001$.

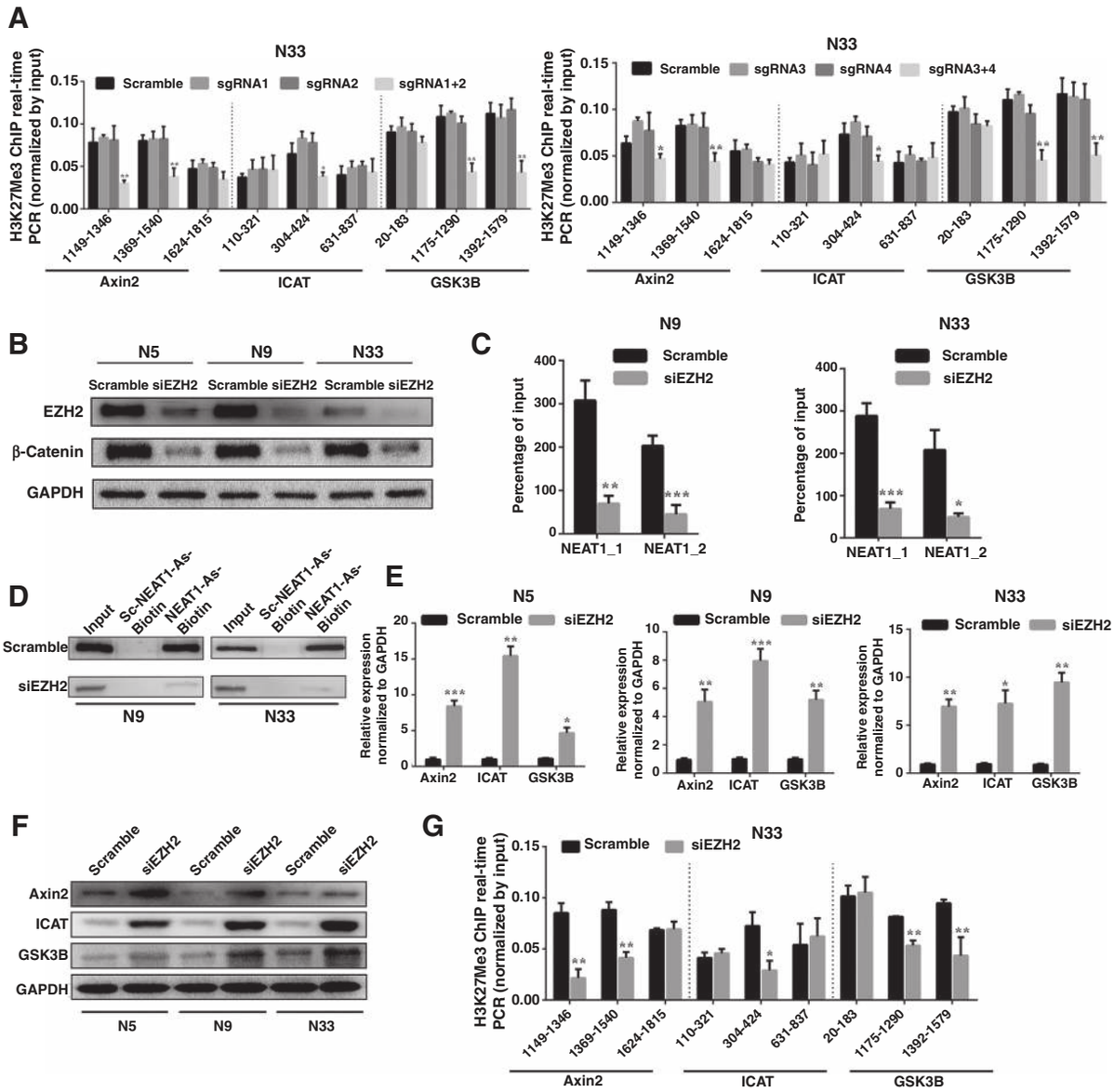

Figure 5.

NEAT1 interacts with EZH2, leading to the trimethylation of H3K27 in the promoter regions of *Axin2*, *ICAT*, and *GSK3B* in glioblastoma. **A,** ChIP-qPCR showed H3K27Me3 occupancy levels in the *Axin2*, *ICAT*, and *GSK3B* promoter regions in different *NEAT1* treatment groups. **B,** The protein levels of EZH2 and β-catenin were detected in the scramble and siEZH2 groups. **C,** RIP assay was performed in the scramble and siEZH2 groups. **D,** ChIRP was performed to examine the association of EZH2. **E** and **F,** The mRNA and protein levels of Axin2, ICAT, and GSK3B were detected in the scramble and siRNA groups. **G,** ChIP-qPCR showed H3K27Me3 occupancy levels in the *Axin2*, *ICAT*, and *GSK3B* promoter regions in the scramble and siEZH2 groups. *, $P < 0.05$; **, $P < 0.01$; ***, $P < 0.001$.

ICAT, and GSK3B increased again in the siEZH2 groups (Fig. 5E and F). Downregulation of EZH2 decreased the H3K27Me3 binding ability of the promoter region of Axin2, ICAT, and GSK3B in N33 cells (Fig. 5G). These results showed that *NEAT1* was the scaffold of EZH2, which played an important role in regulating the WNT/β-catenin pathway in glioblastoma cells.

Knockdown of *NEAT1* impedes orthotopic tumor growth *in vivo*

To further verify the role of *NEAT1 in vivo*, we constructed orthotopic mouse models using the N33 cells. In these models, the *NEAT1* downregulated group showed a significant reduction of the intracranial tumor volume compared to the control groups (Fig. 6A). H&E staining displayed that the tumors in the control groups exhibited extensive branch-like growing patterns that spread into the surrounding tissue (Fig. 6B). We used coinjection of the scramble (e.g., GFP) with sgRNA1+2 (e.g., RFP) group cells (for all three cells: N5, N9, N33) to mimic the complexity of this heterogeneous disease. The results showed that *NEAT1* KO group cells were less proliferative and invasive *in vivo* (Fig. 6C). Meanwhile, *NEAT1* expression was markedly decreased (Fig. 6D) in

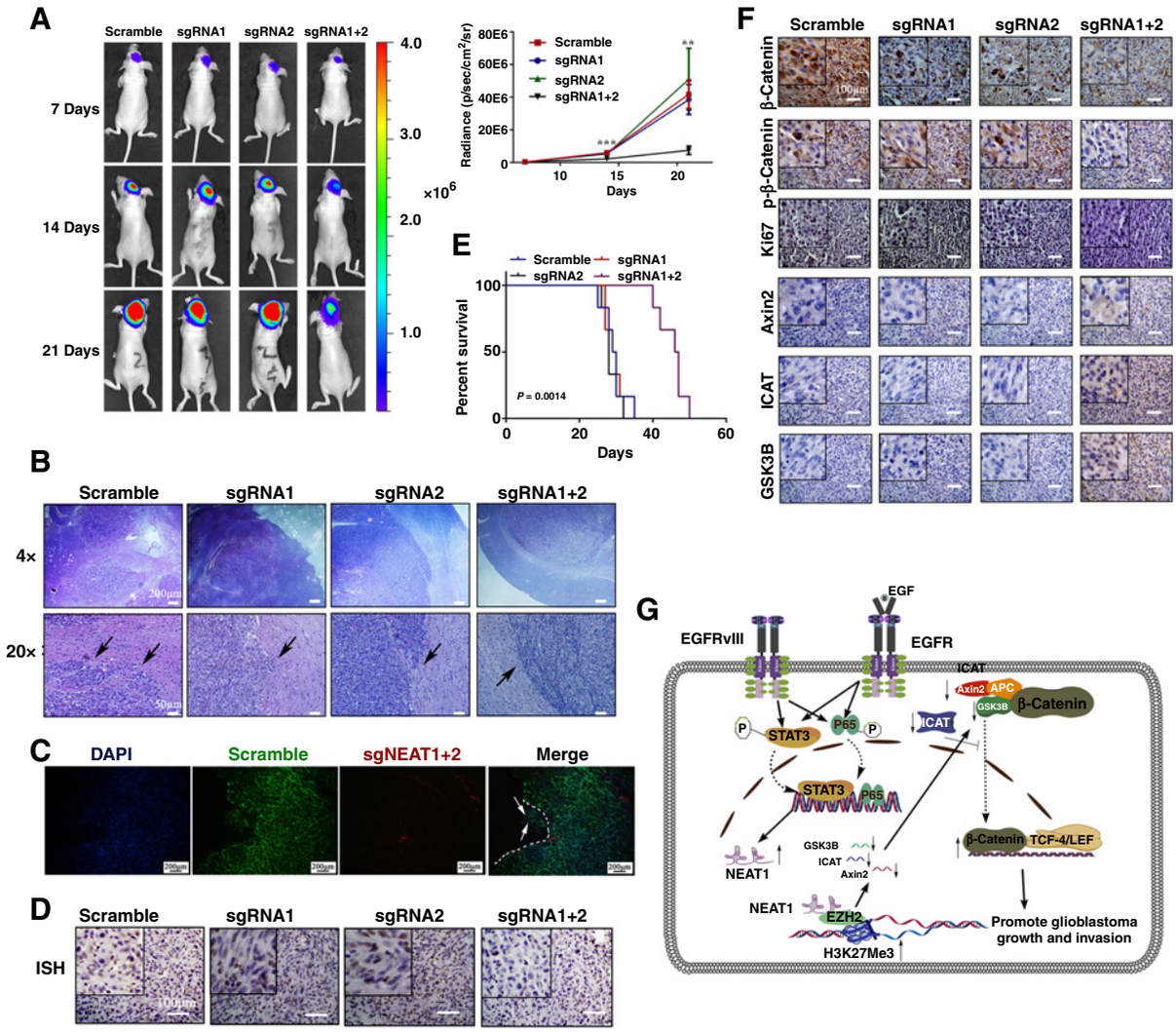

Figure 6.

Knockdown of *NEAT1* in N33 cells impedes orthotopic tumor growth *in vivo*. **A,** Tumor formation was assessed by bioluminescence imaging. **B,** Hematoxylin and eosin staining of the brain tissues from orthotopic mice. **C,** Co-injection of the scramble (GFP) with sgRNA1+2 group cells (RFP; for all three cells: N5, N9, N33) *in vivo*. **D,** RNA ISH for *NEAT1* was measured in mouse paraffin sections. **E,** Kaplan–Meier survival curve was used to determine the overall survival of mice. **F,** Tissue paraffin sections from representative tumors were used for immunohistochemical staining for β-catenin, p-β-catenin, Ki67, Axin2, ICAT, and GSK3B. **G,** Summary of the mechanism of *NEAT1* in glioblastoma. Scale bar, 50, 100, and 200 μm. **, $P < 0.01$; ***, $P < 0.001$.

N33 tumors. Downregulated *NEAT1* in N33 tumors was associated with prolonged survival (Fig. 6E). Furthermore, IHC showed that knockdown of *NEAT1* decreased the expression of β-catenin, p-β-catenin, and Ki-67 but increased the Axin2, ICAT, and GSK3B levels (Fig. 6F) in N33 tumors, consistent with the *in vitro* results.

Discussion

In recent years, by RNA sequencing and annotation by the GENECODE project, thousands of lncRNAs have been discovered, the functions of which have not been established. EGFR module/PDGFR module–based glioma classification forms a framework towards establishing molecular diagnostic tools and identifying novel therapeutic targets to combat gliomas (5). These results indicate that *NEAT1* functions as an oncogene in glioblastoma. In this study, we compared the lncRNA profiles of glioma tissues from different grades using public data sets. We discovered that the lncRNA *NEAT1* was driven by EGFR pathway activity. *NEAT1* is an essential architectural component of paraspeckle nuclear bodies. The tumor anoxia microenvironment can activate *NEAT1* and induce nuclear paraspeckle formation through HIF-2α, leading to breast cancer cell survival (10). In prostate cancer, *NEAT1* has an oncogenic character and alters the epigenetic landscape of target gene promoters to favor transcription (37). *NEAT1* showed the malignant progression in glioma stem cells (38) and clinical significance (23, 24, 39). The results described above strongly prove the oncogenic role of *NEAT1*. In our study, after knocking down *NEAT1* through the dual-CRISPR/Cas9 system, we found that the malignant behaviors of glioblastoma were inhibited.

Next, we sought to identify the underlying molecular mechanisms by which *NEAT1* regulated downstream effectors in glioblastoma. To examine this, we analyzed the differential expression of genes in the CGGA and TCGA data sets. Here, we discovered that the WNT/β-catenin pathway was affected by *NEAT1*. The WNT/β-catenin signaling pathway is associated with diverse processes that are involved in early embryonic patterning and regulation of stem cell self-renewal and differentiation (40). It is not strange that the WNT/β-catenin signal is found in diverse cancers because the aberrant regulation of WNT has a dramatic effect on cell differentiation and fate decisions. Our previous study showed that β-catenin/TCF-4 activity regulated AKT1 expression by binding to the *AKT1* promoter, thereby increasing glioblastoma cell growth (41). In 2012, our laboratory used ChIP-seq assay of TCF4 and STAT3 and data mining of patient cohorts to derive the molecular subtypes of GBM (42). Moreover, the lncRNA *MALAT1* has been reported to be regulated in non-canonical WNT/Ca^{2+}/ signaling (43). In this study, we disclosed that a high level of *NEAT1* negatively regulated WNT negative signaling regulation factors (Axin2, ICAT, and GS3KB). A previous study demonstrated that ICAT is a WNT/β-catenin pathway inhibitor (44). Axin2 itself is a direct target of the WNT signaling pathway and therefore serves to control the duration and/or intensity of WNT signaling through a negative feedback loop (45). GSK3B could form a destruction complex with APC, AXIN, and CSNK1A1, so that β-catenin is phosphorylated at Ser33, Ser37, and Thr41, leading to its ubiquitination by bTRCP and degradation by the proteasome (46). In head and neck squamous cell carcinoma (HNSCC), the loss of GSK3B expression results in the stabilization and accumulation of c-MYC and aggressive HNSCC (47). Our TCF reporter activity, Western blot analysis and immunofluorescence results confirmed that knockdown of *NEAT1* repressed the WNT/β-catenin pathway activity through down-regulating the mRNA and protein levels of ICAT, GSK3B, and Axin2.

To investigate how *NEAT1* regulated the WNT/β-catenin pathway, we found that *NEAT1* was a conserved lncRNA in different species and EZH2 was a potential *NEAT1*-binding protein. It was discovered that the lncRNA *HOTAIR* mediates its effect by interacting with PRC2 though 1 to 500′, enhancing the methylation of histone H3 lysine 27 (H3K27) and leading to the silencing of glioblastoma suppressor genes (48). The expression of EZH2 is high in high-grade glioma, promoting glioma progression, invasion, and metastasis (49). Thus, it was necessary to investigate whether *NEAT1* could bind to EZH2 to silence suppressor gene expression. As we expected, our RNA immunoprecipitation and ChIRP results showed that *NEAT1* interacted with EZH2 in glioblastoma cancer cell lines *in vitro*. Knockdown of *NEAT1* decreased the trimethylation modification of H3K27 in the *Axin2*, *ICAT*, and *GSK3B* promoter region. Finally, our *in vivo* experiments showed tumor growth and invasion were inhibited and mouse lifespan was prolonged after *NEAT1* was knocked down.

In summary, our current work revealed that the glioblastoma-associated lncRNA *NEAT1* was an oncogenic factor that was regulated by EGFR pathway, promoting tumorigenesis by serving as a scaffold and recruiting the chromosome modification enzyme EZH2 to silence target-specific genes (Axin2, ICAT and GSK3B) to promote β-catenin nuclear transport. Thus, the WNT/β-catenin pathway was rekindled in glioblastoma (Fig. 6G). In conclusion, we highlighted that the EGFR/*NEAT1*/EZH2/β-catenin axis in glioblastoma conferred an oncogenic function in glioblastoma that might offer a novel therapeutic target.

Disclosure of Potential Conflicts of Interest

No potential conflicts of interest were disclosed.

Authors' Contributions

Conception and design: C. Kang, M. Li, C. Jiang
Development of methodology: Q. Chen, Y. Wang, C. Kang, C. Jiang
Acquisition of data (provided animals, acquired and managed patients, provided facilities, etc.): Q. Chen, J. Cai, C. Jiang
Analysis and interpretation of data (e.g., statistical analysis, biostatistics, computational analysis): Q. Chen, J. Cai, J. Yang, M. Li, C. Jiang
Writing, review, and/or revision of the manuscript: Q. Chen, J. Cai, Q. Wang, M. Liu, J. Yang, C. Kang, M. Li, C. Jiang
Administrative, technical, or material support (i.e., reporting or organizing data, constructing databases): Q. Chen, J. Cai, Q. Wang, Y. Wang, J. Zhou, C. Kang, C. Jiang
Study supervision: C. Kang, M. Li, C. Jiang

Acknowledgments

The authors thank Professor Xiaolong Fan for the patient-derived cells and Professor Tao Jiang for providing support of data and bioinformatics analysis. This research work was supported by the Research Special Fund for Public Welfare Industry of Health (no. 201402008), the National Key Research and Development Plan (no. 2016YFC0902502), and the National Natural Science Foundation of China (no. 81572701, 81372700, 81702972).

The costs of publication of this article were defrayed in part by the payment of page charges. This article must therefore be hereby marked *advertisement* in accordance with 18 U.S.C. Section 1734 solely to indicate this fact.

Received March 1, 2017; revised June 4, 2017; accepted November 8, 2017; published OnlineFirst November 14, 2017.

References

1. Stupp R, Mason WP, van den Bent MJ, Weller M, Fisher B, Taphoorn MJ, et al. Radiotherapy plus concomitant and adjuvant temozolomide for glioblastoma. N Engl J Med 2005;352:987–96.
2. Brennan CW, Verhaak RG, McKenna A, Campos B, Noushmehr H, Salama SR, et al. The somatic genomic landscape of glioblastoma. Cell 2013;155:462–77.
3. Eskilsson E, Rosland GV, Talasila KM, Knappskog S, Keunen O, Sottoriva A, et al. EGFRvIII mutations can emerge as late and heterogenous events in glioblastoma development and promote angiogenesis through Src activation. Neuro Oncol 2016;18:1644–55.
4. Wong AJ, Ruppert JM, Bigner SH, Grzeschik CH, Humphrey PA, Bigner DS, et al. Structural alterations of the epidermal growth factor receptor gene in human gliomas. Proc Natl Acad Sci U S A 1992;89:2965–9.
5. Sun Y, Zhang W, Chen D, Lv Y, Zheng J, Lilljebjorn H, et al. A glioma classification scheme based on coexpression modules of EGFR and PDGFRA. Proc Natl Acad Sci U S A 2014;111:3538–43.
6. Pastori C, Kapranov P, Penas C, Peschansky V, Volmar CH, Sarkaria JN, et al. The Bromodomain protein BRD4 controls HOTAIR, a long noncoding RNA essential for glioblastoma proliferation. Proc Natl Acad Sci U S A 2015;112:8326–31.
7. Mineo M, Ricklefs F, Rooj AK, Lyons SM, Ivanov P, Ansari KI, et al. The long non-coding RNA HIF1A-AS2 facilitates the maintenance of mesenchymal glioblastoma stem-like cells in hypoxic niches. Cell Rep 2016;15:2500–9.
8. Wang Q, Zhang J, Liu Y, Zhang W, Zhou J, Duan R, et al. A novel cell cycle-associated lncRNA, HOXA11-AS, is transcribed from the 5-prime end of the HOXA transcript and is a biomarker of progression in glioma. Cancer Lett 2016;373:251–9.

9. Clemson CM, Hutchinson JN, Sara SA, Ensminger AW, Fox AH, Chess A, et al. An architectural role for a nuclear noncoding RNA: NEAT1 RNA is essential for the structure of paraspeckles. Mol Cell 2009;33:717–26.
10. Choudhry H, Albukhari A, Morotti M, Haider S, Moralli D, Smythies J, et al. Tumor hypoxia induces nuclear paraspeckle formation through HIF-2alpha dependent transcriptional activation of NEAT1 leading to cancer cell survival. Oncogene 2015;34:4482–90.
11. Adriaens C, Standaert L, Barra J, Latil M, Verfaillie A, Kalev P, et al. p53 induces formation of NEAT1 lncRNA-containing paraspeckles that modulate replication stress response and chemosensitivity. Nat Med 2016;22:861–8.
12. Blume CJ, Hotz-Wagenblatt A, Hullein J, Sellner L, Jethwa A, Stolz T, et al. p53-dependent non-coding RNA networks in chronic lymphocytic leukemia. Leukemia 2015;29:2015–23.
13. Imamura K, Imamachi N, Akizuki G, Kumakura M, Kawaguchi A, Nagata K, et al. Long noncoding RNA NEAT1-dependent SFPQ relocation from promoter region to paraspeckle mediates IL8 expression upon immune stimuli. Mol Cell 2014;53:393–406.
14. XianGuo C, ZongYao H, Jun Z, Song F, GuangYue L, LiGang Z, et al. Promoting progression and clinicopathological significance of NEAT1 over-expression in bladder cancer. Oncotarget 2016. doi: org/10.18632/oncotarget.10084.
15. Wu Y, Yang L, Zhao J, Li C, Nie J, Liu F, et al. Nuclear-enriched abundant transcript 1 as a diagnostic and prognostic biomarker in colorectal cancer. Mol Cancer 2015;14:191.
16. Li Y, Li Y, Chen W, He F, Tan Z, Zheng J, et al. NEAT expression is associated with tumor recurrence and unfavorable prognosis in colorectal cancer. Oncotarget 2015;6:27641–50.
17. Lu Y, Li T, Wei G, Liu L, Chen Q, Xu L, et al. The long non-coding RNA NEAT1 regulates epithelial to mesenchymal transition and radioresistance in through miR-204/ZEB1 axis in nasopharyngeal carcinoma. Tumour Biol 2016;37:11733–41.
18. Ahmad I, Morton JP, Singh LB, Radulescu SM, Ridgway RA, Patel S, et al. beta-Catenin activation synergizes with PTEN loss to cause bladder cancer formation. Oncogene 2011;30:178–89.
19. Zhang K, Zhu S, Liu Y, Dong X, Shi Z, Zhang A, et al. ICAT inhibits glioblastoma cell proliferation by suppressing Wnt/beta-catenin activity. Cancer Lett 2015;357:404–11.
20. Domingues MJ, Rambow F, Job B, Papon L, Liu W, Larue L, et al. beta-catenin inhibitor ICAT modulates the invasive motility of melanoma cells. Cancer Res 2014;74:1983–95.
21. Rosenbluh J, Wang X, Hahn WC. Genomic insights into WNT/beta-catenin signaling. Trends Pharmacol Sci 2014;35:103–9.
22. Zhou X, Ren Y, Moore L, Mei M, You Y, Xu P, et al. Downregulation of miR-21 inhibits EGFR pathway and suppresses the growth of human glioblastoma cells independent of PTEN status. Lab Invest 2010;90:144–55.
23. Du Z, Fei T, Verhaak RG, Su Z, Zhang Y, Brown M, et al. Integrative genomic analyses reveal clinically relevant long noncoding RNAs in human cancer. Nat Struct Mol Biol 2013;20:908–13.
24. Reon BJ, Anaya J, Zhang Y, Mandell J, Purow B, Abounader R, et al. Expression of lncRNAs in low-grade gliomas and glioblastoma multiforme: an in silico analysis. PLoS Med 2016;13:e1002192.
25. Lennox KA, Behlke MA. Cellular localization of long non-coding RNAs affects silencing by RNAi more than by antisense oligonucleotides. Nucleic Acids Res 2016;44:863–77.
26. Ho TT, Zhou N, Huang J, Koirala P, Xu M, Fung R, et al. Targeting non-coding RNAs with the CRISPR/Cas9 system in human cell lines. Nucleic Acids Res 2015;43:e17.
27. Aparicio-Prat E, Arnan C, Sala I, Bosch N, Guigo R, Johnson R. DECKO: single-oligo, dual-CRISPR deletion of genomic elements including long non-coding RNAs. BMC Genomics 2015;16:846.
28. Goyal A, Myacheva K, Gross M, Klingenberg M, Duran Arque B, Diederichs S. Challenges of CRISPR/Cas9 applications for long non-coding RNA genes. Nucleic Acids Res 2017;45:e12.
29. Zhang N, Wei P, Gong A, Chiu WT, Lee HT, Colman H, et al. FoxM1 promotes beta-catenin nuclear localization and controls Wnt target-gene expression and glioma tumorigenesis. Cancer Cell 2011;20:427–42.
30. Ha NC, Tonozuka T, Stamos JL, Choi HJ, Weis WI. Mechanism of phosphorylation-dependent binding of APC to beta-catenin and its role in beta-catenin degradation. Mol Cell 2004;15:511–21.
31. Diederichs S. The four dimensions of noncoding RNA conservation. Trends Genet 2014;30:121–3.
32. Sun M, Nie F, Wang Y, Zhang Z, Hou J, He D, et al. LncRNA HOXA11-AS promotes proliferation and invasion of gastric cancer by scaffolding the chromatin modification factors PRC2, LSD1, and DNMT1. Cancer Res 2016;76:6299–310.
33. Hirata H, Hinoda Y, Shahryari V, Deng G, Nakajima K, Tabatabai ZL, et al. Long noncoding RNA MALAT1 promotes aggressive renal cell carcinoma through Ezh2 and interacts with miR-205. Cancer Res 2015;75:1322–31.
34. Gupta RA, Shah N, Wang KC, Kim J, Horlings HM, Wong DJ, et al. Long non-coding RNA HOTAIR reprograms chromatin state to promote cancer metastasis. Nature 2010;464:1071–6.
35. Tsai MC, Manor O, Wan Y, Mosammaparast N, Wang JK, Lan F, et al. Long noncoding RNA as modular scaffold of histone modification complexes. Science 2010;329:689–93.
36. Zhang K, Sun X, Zhou X, Han L, Chen L, Shi Z, et al. Long non-coding RNA HOTAIR promotes glioblastoma cell cycle progression in an EZH2 dependent manner. Oncotarget 2015;6:537–46.
37. Chakravarty D, Sboner A, Nair SS, Giannopoulou E, Li R, Hennig S, et al. The oestrogen receptor alpha-regulated lncRNA NEAT1 is a critical modulator of prostate cancer. Nat Commun 2014;5:5383.
38. Gong W, Zheng J, Liu X, Ma J, Liu Y, Xue Y. Knockdown of NEAT1 restrained the malignant progression of glioma stem cells by activating microRNA let-7e. Oncotarget 2016;7:62208–23.
39. He C, Jiang B, Ma J, Li Q. Aberrant NEAT1 expression is associated with clinical outcome in high grade glioma patients. APMIS 2016;124:169–74.
40. Grigoryan T, Wend P, Klaus A, Birchmeier W. Deciphering the function of canonical Wnt signals in development and disease: conditional loss- and gain-of-function mutations of beta-catenin in mice. Genes Dev 2008;22:2308–41.
41. Chen L, Huang K, Han L, Shi Z, Zhang K, Pu P, et al. Beta-catenin/Tcf-4 complex transcriptionally regulates AKT1 in glioma. Int J Oncol 2011;39:883–90.
42. Zhang JX, Zhang J, Yan W, Wang YY, Han L, Yue X, et al. Unique genome-wide map of TCF4 and STAT3 targets using ChIP-seq reveals their association with new molecular subtypes of glioblastoma. Neuro Oncol 2013;15:279–89.
43. Vassallo I, Zinn P, Lai M, Rajakannu P, Hamou MF, Hegi ME. WIF1 re-expression in glioblastoma inhibits migration through attenuation of non-canonical WNT signaling by downregulating the lncRNA MALAT1. Oncogene 2016;35:12–21.
44. Tago K, Nakamura T, Nishita M, Hyodo J, Nagai S, Murata Y, et al. Inhibition of Wnt signaling by ICAT, a novel beta-catenin-interacting protein. Genes Dev 2000;14:1741–9.
45. Jho EH, Zhang T, Domon C, Joo CK, Freund JN, Costantini F. Wnt/beta-catenin/Tcf signaling induces the transcription of Axin2, a negative regulator of the signaling pathway. Mol Cell Biol 2002;22:1172–83.
46. Klaus A, Birchmeier W. Wnt signalling and its impact on development and cancer. Nat Rev Cancer 2008;8:387–98.
47. Georgy SR, Cangkrama M, Srivastava S, Partridge D, Auden A, Dworkin S, et al. Identification of a novel proto-oncogenic network in head and neck squamous cell carcinoma. J Natl Cancer Inst 2015;107.
48. Zhou X, Ren Y, Zhang J, Zhang C, Zhang K, Han L, et al. HOTAIR is a therapeutic target in glioblastoma. Oncotarget 2015;6:8353–65.
49. Zhang J, Chen L, Han L, Shi Z, Zhang J, Pu P, et al. EZH2 is a negative prognostic factor and exhibits pro-oncogenic activity in glioblastoma. Cancer Lett 2015;356:929–36.